

Quantum oscillations in the mixed state of d-wave superconductors

Ashot Melikyan¹ and Oskar Vafek²

¹*Materials Science Division, Argonne National Laboratory, Argonne, IL, 60439*

²*National High Magnetic Field Laboratory and Department of Physics,
Florida State University, Tallahassee, Florida 32306, USA*

(Dated: February 9, 2022)

We show that the low-energy density of quasiparticle states in the mixed state of ultra-clean d -wave superconductors is characterized by pronounced quantum oscillations in the regime where the cyclotron frequency $\hbar\omega_c \ll \Delta_0$, the d -wave pairing gap. Such oscillations as a function of magnetic field B are argued to be due to the internodal scattering of the d -wave quasiparticles near wavevectors $(\pm k_D, \pm k_D)$ by the vortex lattice as well as their Zeeman coupling. The periodicity of the oscillations is set by the condition $k_D \sqrt{\hbar c / (eB)} \equiv k_D' \sqrt{\hbar c / (eB')} \pmod{2\pi}$. We find that there is additional structure within each period which grows in complexity as the Dirac node anisotropy increases.

The behavior of d -wave superconductors in magnetic field has recently come into sharp focus due to the experimental observation of the oscillations in the longitudinal and Hall electrical transport at extremely high magnetic fields for very clean underdoped $\text{YBa}_2\text{Cu}_3\text{O}_{6.5}$ [1] and $\text{YBa}_2\text{Cu}_4\text{O}_8$ [2, 3]. At temperatures about 2 K and for magnetic fields in excess of about 30 T, the Hall resistance is finite, *negative* (i.e. electron like), and oscillates as a function of magnetic field, with approximately four pronounced peaks between ~ 45 T and 60 T. Below about 30 T, the system is in the mixed superconducting state, and the electrical Hall conductivity vanishes. The current interpretation of these oscillations involves charge or spin order induced reconstruction of the Fermi surface with electron pockets ([1, 3, 4, 5, 6]), which result from the appropriate tuning of the strength of the charge/spin potentials in the particle-hole channel [4, 5, 6].

As the estimated mean-field H_{c2} for the YBCO samples in question significantly exceeds 60 T [7], it is at present unclear why one should expect the superconducting order parameter amplitude to collapse at the fields applied in Refs. [1, 2, 3]. Instead, the local superconducting correlations should persist, and rather the system is expected to be in the vortex liquid state [8, 9]. Additionally, the sign reversal of the Hall effect, from positive to negative, with decreasing temperature near T_c in optimally doped YBCO has been observed and interpreted earlier as resulting from the flux flow [10, 11, 12]. The structure factor of such liquid state is expected to closely resemble that of a vortex solid. In this context, the natural question is the existence, the periodicity, and the physical nature of such magnetic field induced oscillations in the vortex state.

In this work we therefore examine the properties of the d -wave quasiparticles (qps) in the vortex solid state at intermediate magnetic fields, i.e. we examine the particle-particle channel. For the square vortex lattice observed in the small angle neutron scattering [13], we find that the combined effect of the orbital and spin coupling of the qps to the magnetic field does induce os-

illations in the low energy density of states, $N(E)$, and that the nature of these oscillations depends on the Dirac cone anisotropy α_D . In the physically relevant regime where the d -wave gap $\Delta_0 \gg \hbar\omega_c$ (the cyclotron frequency $\omega_c = eB/mc$), the density of states $N(E)$ is an oscillatory function of $k_D\ell$, where k_D is the k -space half-distance between the nearest nodes (see Fig. 1) and ℓ is the magnetic length $\ell = \sqrt{\hbar c / Be}$. For $\alpha_D = 1$, the period of the oscillations corresponds to $\delta(k_D\ell) = 2\pi$, but with increasing anisotropy the number of oscillations *within* the period increases. In the absence of Zeeman coupling $N(E)$ is exactly periodic in the scaling regime and the spectrum oscillates between fully gapped and nodal. Upon inclusion of the Zeeman coupling, which cannot be neglected for fields of Ref. [1, 2, 3], the oscillatory behavior persists, but the scaling is only approximate. For $\alpha_D = 1$ and for the fields in the excess of $30T$, the combined effect of the orbital and Zeeman coupling leads to a sequence of transitions and the system oscillates between a thermal metal with finite $N(0)$ and a thermal insulator with vanishing $N(0)$. A similar pattern of oscillating behavior holds for large α_D , albeit with effectively increased frequency and significantly decreased gap. The envelope of the $N(0)$ oscillations follows an approximately ℓ^{-1} behavior. These findings should be contrasted with the oscillations found in the regime of extreme high fields Ref. [14] where the number of Landau levels below the Fermi energy range from 1 to 7.

The starting point is the lattice Bogoliubov-de Gennes (BdG) eigenequation [15, 16]

$$\hat{\mathcal{H}}_0 \psi_{\mathbf{r}} = E \psi_{\mathbf{r}}. \quad (1)$$

where the Hamiltonian $\hat{\mathcal{H}}_0$ acts on the two component Nambu spinor $\psi_{\mathbf{r}} = [u_{\mathbf{r}}, v_{\mathbf{r}}]^T$ and has the following explicit form

$$\hat{\mathcal{H}}_0 = \begin{pmatrix} \hat{\mathcal{E}}_{\mathbf{r}} - \mu + \frac{q}{2}\mu_B B & \hat{\Delta}_{\mathbf{r}} \\ \hat{\Delta}_{\mathbf{r}}^* & -\hat{\mathcal{E}}_{\mathbf{r}}^* + \mu + \frac{q}{2}\mu_B B \end{pmatrix}. \quad (2)$$

Both $\hat{\mathcal{E}}_{\mathbf{r}}$ and $\hat{\Delta}_{\mathbf{r}}$ are defined through their action on a

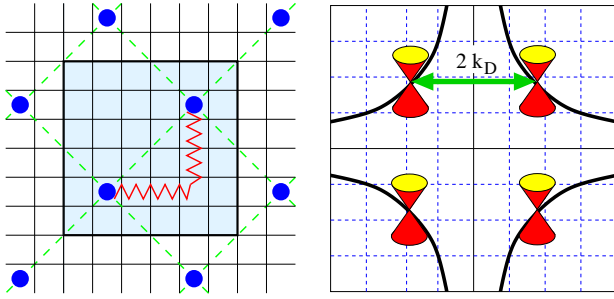


FIG. 1: Left: Magnetic unit cell $\ell \times \ell$ of a tight-binding lattice (solid lines) containing two vortices joined by a branch-cut shown for $\ell = 6a$. Right: Fermi surface (black solid lines) of cuprate superconductors with four nodal points at $\mathbf{k}_F^{(j)} = (\pm k_D, \pm k_D)$ in a Brillouin zone of size $2\pi/a$. In the presence of the vortex lattice, the Brillouin zone is reduced to $2\pi/\ell$ (spacing of the blue grid). The properties of the low energy states depend on the commensuration between the inter-nodal distance $2k_N$ and the reduced reciprocal lattice vector $2\pi/\ell$.

lattice function $f_{\mathbf{r}}$ as

$$\hat{\mathcal{E}}_{\mathbf{r}} f_{\mathbf{r}} = -t \sum_{\delta=\pm\hat{x},\pm\hat{y}} e^{-i\mathbf{A}_{\mathbf{r}\mathbf{r}+\delta}} f_{\mathbf{r}+\delta}, \quad (3)$$

$$\hat{\Delta}_{\mathbf{r}} f_{\mathbf{r}} = \Delta_0 \sum_{\delta=\pm\hat{x},\pm\hat{y}} e^{i\theta_{\mathbf{r}\mathbf{r}+\delta}} \eta_{\delta} f_{\mathbf{r}+\delta}. \quad (4)$$

In the symmetric gauge, the magnetic flux Φ through an elementary plaquette enters the Peierls factor via $\mathbf{A}_{\mathbf{r}\mathbf{r}+\hat{x}} = -\pi y \Phi / \phi_0$, $\mathbf{A}_{\mathbf{r}\mathbf{r}+\hat{y}} = \pi x \Phi / \phi_0$; the electronic flux quantum is $\phi_0 = hc/e$. The d -wave symmetry is encoded in $\eta_{\delta} = +(-)$ if $\delta \parallel \hat{\mathbf{x}}(\hat{\mathbf{y}})$. Importantly, $\theta_{\mathbf{r}\mathbf{r}'}$ winds by 2π around each of the magnetic field induced vortices. The initial Ansatz[17] for the pair phases is

$$e^{i\theta_{\mathbf{r}\mathbf{r}'}} \equiv (e^{i\phi_{\mathbf{r}}} + e^{i\phi_{\mathbf{r}'}}) / |e^{i\phi_{\mathbf{r}}} + e^{i\phi_{\mathbf{r}'}}|, \quad (5)$$

where $\nabla \times \nabla \phi(\mathbf{r}) = 2\pi \hat{\mathbf{z}} \sum_i \delta(\mathbf{r} - \mathbf{r}_i)$ and $\nabla \cdot \nabla \phi(\mathbf{r}) = 0$ where \mathbf{r}_i denotes the vortex positions. Although the phase of the order parameter does depend on the precise form of the self-consistency condition, the deviations from the adopted form are weak, and moreover, both the symmetry of the phase and its singular part are fixed unambiguously by the vortex lattice.

Connecting pairs of vortices by branch cuts[17], we can define the singular gauge transformation[17, 18] $\mathcal{U} = e^{\frac{i}{2}\sigma_3 \phi}$ where the Pauli sigma matrices act on the Nambu spinors. The transformed Hamiltonian $\mathcal{H}(\mathbf{k}) = e^{-i\mathbf{k}\cdot\mathbf{r}} \mathcal{U}^{-1} \hat{\mathcal{H}}_0 \mathcal{U} e^{i\mathbf{k}\cdot\mathbf{r}}$ becomes

$$\mathcal{H}(\mathbf{k}) = \sigma_3 \left(\tilde{\mathcal{E}}_{\mathbf{r}}(\mathbf{k}) - \mu \right) + \sigma_1 \tilde{\Delta}_{\mathbf{r}}(\mathbf{k}) + \frac{g}{2} \mu_B B, \quad (6)$$

where the transformed lattice operators satisfy

$$\tilde{\mathcal{E}}_{\mathbf{r}}(\mathbf{k}) \psi_{\mathbf{r}} = -t \sum_{\delta=\pm\hat{x},\pm\hat{y}} z_{2,\mathbf{r}\mathbf{r}+\delta} \times e^{i\sigma_3 V_{\mathbf{r}\mathbf{r}+\delta}} e^{i\mathbf{k}\cdot\delta} \psi_{\mathbf{r}+\delta} \quad (7)$$

$$\tilde{\Delta}_{\mathbf{r}}(\mathbf{k}) \psi_{\mathbf{r}} = \Delta_0 \sum_{\delta=\pm\hat{x},\pm\hat{y}} z_{2,\mathbf{r}\mathbf{r}+\delta} \times \eta_{\delta} e^{i\mathbf{k}\cdot\delta} \psi_{\mathbf{r}+\delta}. \quad (8)$$

The physical superfluid velocity enters via the factor

$$e^{iV_{\mathbf{r}\mathbf{r}'}} = e^{-i\mathbf{A}_{\mathbf{r}\mathbf{r}'}} (1 + e^{i(\phi_{\mathbf{r}'} - \phi_{\mathbf{r}})}) / |1 + e^{i(\phi_{\mathbf{r}'} - \phi_{\mathbf{r}})}| \quad (9)$$

and represents the lattice analog of the semiclassical (Doppler) effect[19]. The Z_2 field $z_{2,\mathbf{r}\mathbf{r}'} = 1$ on each bond except the ones crossing the branch cut where $z_{2,\mathbf{r}\mathbf{r}'} = -1$.

In the magnetic fields of interest the vortices of YBCO form a square lattice with primitive vectors oriented along the d -wave nodes[13], and therefore the transformed Hamiltonian (6) is invariant under discrete translations by the primitive vectors $\mathbf{R}_1 = \ell \hat{x}$ and $\mathbf{R}_2 = \ell \hat{y}$ defining the magnetic unit cell, reflecting the periodicity of $V_{\mathbf{r}\mathbf{r}'}$ and the periodic choice of the branch cuts. Consequently, it can be diagonalized in the Bloch basis. By the Bloch condition $\mathcal{H}(\mathbf{k})$ acts on the periodic functions, and the crystal wavevector \mathbf{k} varies continuously within the 1st Brillouin zone defined by the primitive reciprocal lattice vectors $\mathbf{K}_1 = 2\pi \frac{\hat{x}}{\ell}$, $\mathbf{K}_2 = 2\pi \frac{\hat{y}}{\ell}$. Note that, since the unitary transformation \mathcal{U} is time independent, the Hamiltonians (2) and (6) have the same thermodynamic and tunneling density of states.

The above claims follow from our detailed numerical study of the tight-binding Bogoliubov-de Gennes Hamiltonian (6). Since the Zeeman term is just a simple overall shift of the qp energies, let us first neglect it. The results of the numerical diagonalization of (6) can be summarized by the following scaling form of the qp eigenenergies:

$$E_n(\mathbf{k}) = \frac{\hbar v_F}{\ell} \mathcal{F}_n(\mathbf{k}\ell, \alpha_D, k_D \ell). \quad (10)$$

Here v_F and v_{Δ} are the Fermi and gap velocities of the d -wave qps near the nodes $(\pm k_D, \pm k_D)$ (in our model (2) $v_F = 2\sqrt{2} a \hbar^{-1} \sin(k_D a)$ and $v_{\Delta} = v_F \Delta_0 / t$); \mathcal{F}_n is a dimensionless scaling function, which differs from the Simon-Lee scaling function in the following important aspect: it depends on $k_D \ell$. Specifically, in the scaling limit of $k_D \ell \rightarrow \infty$, the function \mathcal{F}_n does not approach a uniform value. This is amply illustrated in the Fig.(2), where we used a color density plot to represent the density of states per area rescaled as $v_F \ell N(E)$ for different values of $k_D \ell / (2\pi)$ and $E \ell / (\hbar v_F)$.

As best seen for $\alpha_D = 1$, near $E = 0$ the spectrum is gapped although for $k_D \ell \approx \pi(2n + 1)$ the gap is very small, vanishing only at discrete set of points as expected for the unitary class[16]. Moreover, the gap scales as ℓ^{-1} and oscillates as a function of $k_D \ell$. Physically, the oscillations are due to the strong internodal scattering which arises from the commensurability of the d -wave nodes and the vortex lattice. As seen from the three different panels, the pattern of the oscillations depends on the anisotropy α_D . With increasing α_D , the DOS acquires ever richer structure with multiple minima and maxima – for presentation purposes we show only three periods

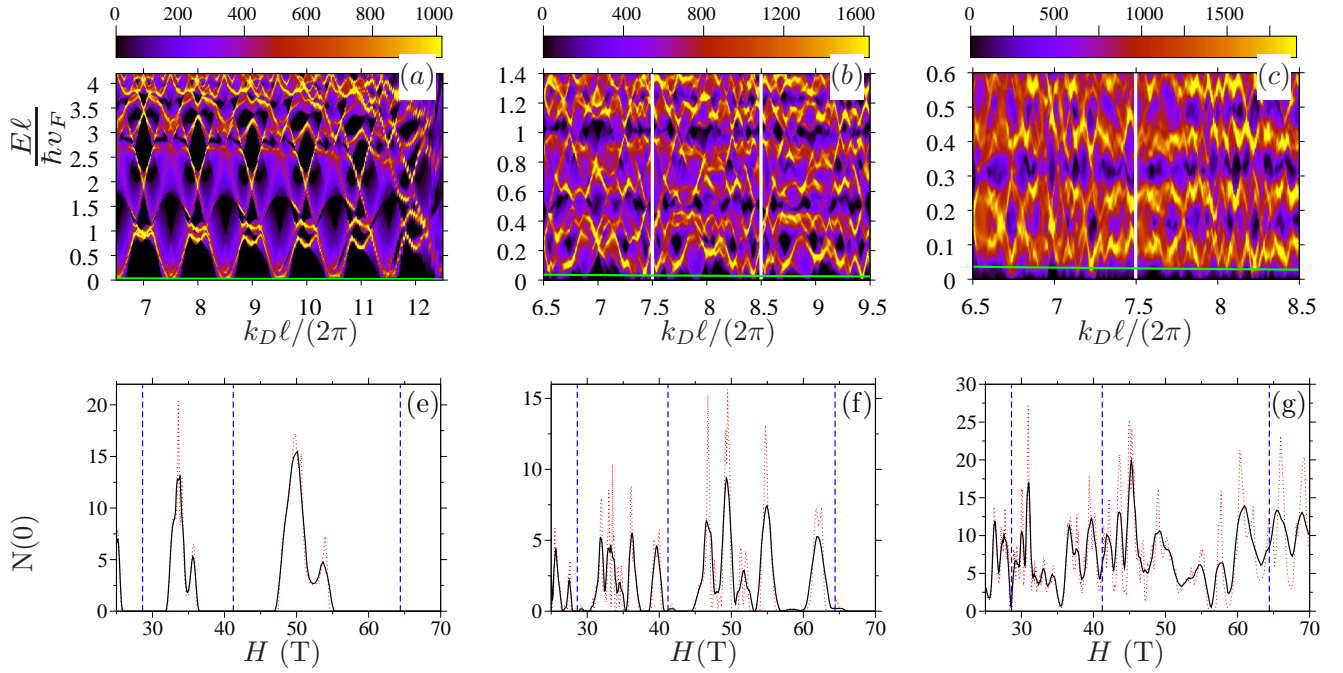


FIG. 2: (a-c): Oscillations of the qp density of states $N(E)$ rescaled as $\ell v_F N(\ell E / (\hbar v_F))$ are shown as a color map for $\alpha_D = 1$ (a), $\alpha_D = 4$ (b), and $\alpha_D = 7$ (c). The green line represents the shift of the qp zero energy due to the Zeeman term for $t = 380$ meV, $a = 3.8$ Å, $g = 2$, $k_D = 0.38\pi/a$, and $\ell = 26a$. (e-f): Zero energy density of states of (2) as a function of magnetic field for $\alpha_D = 1$ (e), 4 (f), 7 (g) deduced from the figures of the top row and the generalized scaling form of eigenvalues (10) is shown in red dashed line. The solid black line corresponds to an effective broadening due to the inter-layer coupling $2t_z \cos(k_z c)$ with $t_z = 0.05t$.

(separated by white vertical lines) for $\alpha_D = 4$ and two periods for $\alpha_D = 7$. Additionally, as α_D increases, the scaling limit $\Delta_0 \gg \hbar\omega_c$ is reached for smaller magnetic fields (larger ℓ) and the approximate low energy scaling (10) holds for magnetic length $\ell/a \gg 2\pi\sqrt{\alpha_D}$.

The magnetic fields of experimental interest (45–70 T) correspond to $\ell \in (20a, 25a)$, which is the regime where the Zeeman term cannot be neglected. Nevertheless, it is easy to take it into account, since it corresponds to a simple shift in zero of the qp energy, represented by the green lines in each of the color DOS maps in Fig. 2. The DOS along the Zeeman "slice" is shown in Figs. 2(e-f). For anisotropy $\alpha_D = 1$, the spectrum exhibits pronounced oscillations as a function of magnetic field (or k_D), changing from gapped (thermal insulator) with activated temperature dependence of the specific heat to gapless (thermal metal) with T -linear specific heat. This $\delta\ell = 2\pi/k_D$ periodic sequence of transitions between thermal metal and thermal insulator is significantly richer for $\alpha_D > 1$. Within each such "primitive" period, a complex structure develops, and the number of minima and maxima depends on α_D . For $\alpha_D = 7$ and $k_D = 0.38\pi/a$, which are approximately [20] the physical values expected for the YBCO samples of Ref. [1], there are four "oscillations" in the field range $\sim 45 - 60T$. Remarkably, this is precisely the experimentally observed "periodicity" [1].

Note that the effect described here occurs deep in vortex state with a fully developed superconducting amplitude and does not rely on semiclassical orbits around electron pockets. Rather, as we now argue, it is a consequence of the commensuration involving the vortex lattice and the internodal separation (see Fig. 1). In the scaling regime of interest, $\Delta_0 \gg \hbar\omega_c$, the appropriate starting point should be the linearized approximation [18, 21] of BdG Hamiltonian (6). In this approach the low-energy qps with $E \ll \Delta_0$ are independent and behave as massless Dirac fermions interacting with vortices via the Doppler shift originating from the superflow $\mathbf{v}(\mathbf{r}) = \frac{\hbar}{2}\nabla\phi - \frac{e}{c}\mathbf{A}$. Additionally, the wavefunctions contain branch-cuts connecting vortices pairwise [16, 17, 18, 21, 22, 23, 24]. The effective Hamiltonian [18, 21, 22, 23] is then

$$\mathcal{H}_{lin}/v_F = \frac{p_x + p_y}{\sqrt{2}}\sigma_3 + \alpha_D \frac{p_y - p_x}{\sqrt{2}}\sigma_1 + m \frac{v_x + v_y}{\sqrt{2}}. \quad (11)$$

In this approximation, \mathcal{H}_{lin} exhibits the Simon-Lee [21] scaling $\mathcal{H}_{lin}(\mathbf{r}, v_F, v_\Delta) = \frac{\hbar v_F}{\ell} \mathcal{H}_{lin}(\mathbf{r}/\ell, \alpha_D, 1)$ and the qp spectrum has a scaling form $E_n(\mathbf{k}) = \frac{\hbar v_F}{\ell} \mathcal{F}_n^{(lin)}(\mathbf{k}\ell, \alpha_D)$.

Now, we consider the corrections due to the terms left out during linearization. Provided that \mathbf{r} is not in the immediate vicinity of a vortex core ($r \gtrsim \xi$), the leading non-linear corrections, such as $m\mathbf{v}^2(\mathbf{r})/2$, are typically

omitted on the basis that they are smaller than the terms retained in (11) by a factor of $(k_D \ell)^{-1}$ which is small for typical fields of interest. However, such estimate is incorrect. The effect of the non-linear terms is amplified[24] by an anomalously large (low energy) qp wavefunctions, growing as $r^{-1/2}$ near vortex locations[16, 25]. This divergence is eventually cut off only at $r \approx \xi$. A typical “perturbation”, such as $m\mathbf{v}^2(\mathbf{r})$, results in the following matrix element between two eigenstates of \mathcal{H}_{lin} at nodes j and j' : $I = \langle \Psi_{n\mathbf{k}}^{(j)} | m\mathbf{v}^2(\mathbf{r}) | \Psi_{n'\mathbf{k}'}^{(j')} \rangle$. Due to Bloch symmetry of the wavefunctions Ψ , the Bloch momenta $\mathbf{k}_F^{(j)} + \mathbf{k}$ and $\mathbf{k}_F^{(j')} + \mathbf{k}'$ must differ by a reciprocal lattice vector \mathbf{G} . Importantly, $|I| \propto \frac{\hbar v_F}{\ell} \frac{1}{k_D \xi} [C_1 + C_2 \cos(\mathbf{R} \cdot \mathbf{G})]$, which is of the same order as the terms retained in (11). Here \mathbf{R} is the primitive vortex lattice vector and the vortex core size ξ serves as the small-distance cut-off of the otherwise divergent integrals[24]. Coefficients $C_{1,2}$, in general depend on \mathbf{k} and \mathbf{k}' , but not on $\mathbf{k}_F^{(j)}$ or $\mathbf{k}_F^{(j')}$.

Thus, due to the $r^{-1/2}$ -behavior of the low-energy wavefunctions near vortex cores, the matrix elements I , and the resulting corrections to the energies, scale with magnetic length precisely as the energies of (11), namely as $\sim \ell^{-1}$. The relative magnitude of the corrections due to the non-linearities compared to (11) is determined by the magnitude of the parameter $(k_D \xi)^{-1}$ rather than $(k_D \ell)^{-1}$. In cuprate superconductors the former is typically of $\mathcal{O}(1)$ since ξ is of the order of a few lattice spacings. Thus, if the parameters of the BdG Hamiltonian (6) such μ or ℓ are varied, the resulting qp spectrum evolves in a manner not captured by (11).

Based on the above argument, for the square vortex lattice under consideration we expect the spectra for nodal momentum k_D (k_D') and magnetic length ℓ (ℓ') to be similar when

$$k_D \ell \equiv k_D' \ell' \pmod{2\pi}. \quad (12)$$

Therefore, the Simon-Lee scaling should be generalized to Eq. (10). In the regime where the scaling (10) holds the oscillatory part of the dispersion is fully determined by the product $k_D \ell$, and therefore the dependence of the spectrum on the magnetic field can be determined from the changes in k_D [24]. Finally, for $\mu = 0$ (or equivalently $k_D = \pi/(2a)$), the characteristic oscillations found in this work can be proven rigorously without appealing to the perturbation theory [17]. In this case, when ignoring the Zeeman coupling, the qp spectrum is gapless when $k_D \ell / (2\pi)$ is a half-integer and gapped when it is an integer.

Since the effect described here is due to the interference effects between the nodal d -wave qps and the ordered vortex positions, it should be observable[26] as long as the thermal length $L_T = \hbar v_F / (k_B T)$ exceeds ℓ . We ex-

pect these oscillations to persist in a vortex liquid state with strong, albeit only short range, positional order, provided that the vortex positional correlation length $\xi_p \gg L_T \gg \ell$. The true test of these predictions, however, would be an observation of the high field quantum oscillations in the low temperature specific heat in the superconducting state with nearly perfect vortex lattice. The two parameters which control the pattern of the oscillations are k_D and α_D , both of which depend on doping and can be determined independently.

We thank Z. Tešanović for useful discussions. A. M. would also like to thank M. Norman for helpful discussions and a critical reading of the manuscript.

A. M. was supported by the U. S. Dept. of Energy, Office of Science, under Contract No. DE-AC02-06CH11357. O. V was supported in part by the NSF grant DMR-00-84173.

-
- [1] N. Doiron-Leyraud *et al.*, Nature **447**, 565 (2007).
 - [2] E. A. Yelland *et al.*, arXiv:0707.0057.
 - [3] A. F. Bangura *et al.*, arXiv:0707.4461.
 - [4] W.-Q. Chen *et al.*, arXiv:0706.3556.
 - [5] A. J. Millis and M. Norman, arXiv:0709.0106.
 - [6] S. Chakravarty and H.-Y. Kee, arXiv:0710.0608.
 - [7] Y. Wang *et al.*, Phys. Rev. Lett. **88**, 257003 (2002).
 - [8] D. A. Huse *et al.*, Nature **358**, 553 (1992).
 - [9] L. Li *et al.*, Nature Physics **3**, 311 (2007).
 - [10] M. Galffy and E. Zirngiebl, Solid State Commun. **68**, 929 (1988).
 - [11] S. J. Hagen *et al.*, Phys. Rev. B **41**, 11630 (1990).
 - [12] T. R. Chien *et al.*, Phys. Rev. Lett. **66**, 3075 (1991).
 - [13] S. P. Brown *et al.*, Phys. Rev. Lett. **92**, 067004 (2004).
 - [14] K. Yasui and T. Kita, Phys. Rev. Lett. **83**, 4168 (1999); Phys. Rev. B **66**, 184516 (2002).
 - [15] Y. Wang and A. H. MacDonald, Phys. Rev. B **52**, R3876 (1995).
 - [16] O. Vafek *et al.*, Phys. Rev. B **63**, 134509 (2001); *ibid.* **64**, 224508 (2001).
 - [17] O. Vafek and A. Melikyan, Phys. Rev. Lett. **96**, 167005 (2006).
 - [18] M. Franz and Z. Tešanović, Phys. Rev. Lett. **84**, 554 (2000).
 - [19] G. E. Volovik, JETP Lett. **58**, 469 (1993).
 - [20] M. Sutherland *et al.*, Phys. Rev. B **67**, 174520 (2003).
 - [21] S. H. Simon and P. A. Lee, Phys. Rev. Lett. **78**, 1548 (1997).
 - [22] L. Marinelli, B. I. Halperin, and S. H. Simon, Phys. Rev. B **62**, 3488 (2000).
 - [23] A. Vishwanath, Phys. Rev. Lett. **87**, 217004 (2001); A. Vishwanath, Phys. Rev. B **66**, 064504 (2002).
 - [24] A. Melikyan and Z. Tešanović, Phys. Rev. B **74**, 144501 (2006); *ibid.* **76**, 094509 (2007).
 - [25] A. S. Mel'nikov, Phys. Rev. Lett. **86**, 4108 (2001).
 - [26] A. Melikyan and O. Vafek, <http://meetings.aps.org/link/BAPS.2007.MAR.A10.3>.